Journal of Pharmaceutical Research International

Volume 36, Issue 6, Page 77-87, 2024; Article no.JPRI.116383
ISSN: 2456-9119, NLM ID: 101716968
(Past name: British Journal of Pharmaceutical Research, Past ISSN: 2231-2919, NLM ID: 101631759)

Bio-fabrication and Characterization of Green Synthesized Nanoparticles from Commercial Honey

Najla Ali Alburae [a*]

[a] *Department of Biological Sciences, King Abdulaziz University, P.O. Box 80206, 21589, Jeddah, Saudi Arabia.*

Author's contribution

The sole author designed, analyzed, interpreted and prepared the manuscript.

Article Information

DOI: 10.9734/JPRI/2024/v36i67524

Open Peer Review History:
This journal follows the Advanced Open Peer Review policy. Identity of the Reviewers, Editor(s) and additional Reviewers, peer review comments, different versions of the manuscript, comments of the editors, etc are available here: https://www.sdiarticle5.com/review-history/116383

Original Research Article

Received: 01/03/2024
Accepted: 02/05/2024
Published: 04/05/2024

ABSTRACT

Green approaches to nanoparticle synthesis offer sustainable and environmentally friendly alternatives, avoiding hazardous chemicals typical in traditional methods. This study characterizes nanoparticles (NPs) synthesized from silver nitrate (AgNO3) and iron oxide (Fe2O3) using commercial honey as a reducing and capping agent. Characterization revealed significant disparities between silver NPs (AgNPs) and iron NPs (FeNPs). AgNPs had a larger particle size (Z-average: 3115.67 nm) compared to FeNPs (Z-average: 1813 nm). AgNPs showed a monodisperse population, while FeNPs had a slightly broader size distribution. Additionally, AgNPs had a higher particle concentration (mean count rate: 505.17 kcps) than FeNPs (mean count rate: 296.65 kcps). Both AgNPs and FeNPs displayed negative surface charges, at -6.499 mV and -1.652 mV, respectively, where FeNPs exhibit a slightly higher value. Elemental composition analysis by scanning electron microscope – energy dispersive X-ray (SEM-EDX) revealed that AgNPs are primarily composed of silver, carbon, and oxygen, whereas FeNPs consisted mainly of iron, oxygen, and carbon. These findings provide insights into the physical and chemical properties of AgNPs and FeNPs synthesized using commercial honey. Understanding these properties is

**Corresponding author: E-mail: nalbourai@kau.edu.sa, nalbourae@gmail.com;*

essential for optimizing synthesis processes and exploring applications in medicine, catalysis, and environmental remediation. The eco-friendly synthesis approach using honey underscores the potential for sustainable nanomaterial production. Further research can explore specific applications and benefits of AgNPs and FeNPs synthesized through this green method, offering an efficient and economical alternative for nanoparticle synthesis.

Keywords: Nanoparticle synthesis; green approach; commercial honey; characterization; AgNPs, FeNPs.

1. INTRODUCTION

Over the past two decades, nanotechnology has garnered considerable attention due to its wide-ranging applications across various scientific domains. Among the myriad nanomaterials, metal oxide nanoparticles (NPs) have emerged as a subject of intensive investigation owing to their distinctive properties [1]. The nanomaterials synthesis employs diverse methods encompassing physical, chemical, and biological routes [2]. At present, metallic NPs are applied in catalysis, sensor technologies, disease diagnosis, and treatment, among other applications [3]. However, traditional physio-chemical processes for nanoparticle production entail drawbacks such as the generation of harmful chemicals, costly equipment, multistep procedures, and the release of toxic by-products [4]. Moreover, techniques such as lithography, laser ablation, aerosol technologies, and ultraviolet irradiation, though effective, remain financially burdensome. Consequently, employing microorganisms and environmentally benign approaches for nanoparticle synthesis has received an increased attention [5]. This shift towards simpler, cost-effective, and eco-friendly techniques is increasingly attractive [6].

The exploration of plant systems for the biologically assisted synthesis of metal NPs, known as green synthesis, stands as a pivotal endeavor in nanoscience research [7]. Studies have demonstrated the efficacy of utilizing fungi, algae, bacteria, and plant extracts for the green synthesis of AgNPs [8]. The development of techniques enabling the controlled synthesis of NPs with precise size, shape, and composition is imperative for their application in diverse fields such as biomedicine, optics, electronics, and water purification [7,8]. Recent reports highlight the use of various plant extracts, including coriander leaf, edible mushrooms, algae, cyanobacteria, and fungi, in the biosynthesis of gold and silver nanoparticles. The versatility of NPs, attributed to their diminutive size of less than 100 nm, underscores their significance [9,10]. Size reduction confers distinctive properties upon NPs, such as increased surface area and enhanced magnetic and electrochemical characteristics [11].

Among metallic NPs, AgNPshave garnered significant attention due to their potent antimicrobial activity compared with macroscopic silver [12,13]. Natural compounds present in various products, such as alkaloids, phenols, tannins, terpenoids, amino acids, and proteins, facilitate the reduction of Ag+ ions to Ag-NPs, there by stabilizing them and preventing aggregation [14–16]. AgNPs exhibit exceptional antimicrobial properties, which have been proven effective against a broad spectrum of pathogens including bacteria, fungi, and viruses. Moreover, iron oxide NPs (Fe_2O_3-NPs), particularly magnetic ones, have gained prominence in applications such as drug delivery, magnetic resonance imaging, and bioremediation [17,18]. Various chemical methods are employed for the synthesis of Fe_2O_3-NPs, with recent studies showcasing successful synthesis using aqueous extracts of plants.

Apis mellifera honey, renowned for its therapeutic properties since ancient times, serves as a natural source of nutrition rich in glucose and fructose. Honey-mediated nanoparticle synthesis offers a biocompatible, rapid, and straightforward approach devoid of hazardous by-products, rendering its suitability for diverse applications [19]. Moreover, honey exhibits numerous health benefits, including antimicrobial, antioxidant, anti-inflammatory, and antiviral properties, further accentuating its potential in nanoparticle synthesis and medical applications.

The present study aimed to synthesize and characterize AgNPs andFeNPs using *Apis mellifera* honey via a green synthesis approach. This endeavor explores the feasibility of utilizing honey as a reducing and capping agent for eco-friendly nanoparticle synthesis at ambient conditions. The approach also aims to evaluate

their physicochemical properties and potential for various nano-biotechnological applications.

2. MATERIALS AND METHODS

2.1 Biosynthesis of the NPs, Silver Nitrate ($AgNO_3$) and Iron Oxide (Fe_2O_3) Using Natural Honey

White velvet mesquite organic honey sourced from *Apis mellifera* (honeybee) was procured from the L'Organic online store (Code: LATINHONEY-FIBHJ-17305). In a typical experiment, 20 g of honey was dissolved in 80 ml of deionized water. To prepare a 1 mM solution of ($AgNO_3$), 0.042 g of $AgNO_3$ (Sigma, CAS No: 7761-88-8) was dissolved in 250 ml of deionized distilled water. Subsequently, 20 mL of the prepared 10-3 M $AgNO_3$ solution was added to 15 mL of the honey solution, and the pH was adjusted to 6.5 using 99% pure NaOH [20].

For the green synthesis of FeNPs, a 50% honey solution and 1 mM $FeCl_3.6H_2O$ (Sigma, CAS No: 10025-77-1; 98% pure) were mixed in a 1:1 ratio in a flask. Then, NaOH (99% pure) was added dropwise to adjust the pH of the solution to 11. Both final solutions were vigorously stirred for 30 minutes on a magnetic stirrer until an intense black colour indicated the formation of Fe_2O_3-NPs, whereas a golden yellow colour indicated the formation of $AgNO_3$-NPs [21]. Centrifugation at 8000 rpm. for 40 minutes was conducted to separate nanoparticles from other particles in the solution. The resulting pellet was washed three times with water and ethanol. An ultrafine powder of NPs was obtained by drying the solution in a hot air oven at 80°C for 6–7 hours [22].

2.2 Nanoparticle Characterization of ($AgNO_3$) and (Fe_2O_3)

Nanomaterials synthesized from silver nitrate and iron oxide were characterized using various analytical techniques. The UV-Vis spectrophotometry was initially performed to determine the spectral frequencies of $AgNO_3$-NPs within the range of 200 nm to 1000 nm and $Fe2O_3$-NPs within the range of 200 nm to 800 nm. Double-beam UV–Vis spectra were measured using a spectrophotometer (model Victoria, Australia) with two quartz cuvettes, one containing water and the other containing approximately 3 mL of each nanomaterial [21]. Pure samples were diluted up to five times to reduce noise, and the experiment was conducted in triplicate for each nanomaterial from the aqueous honey solution. Subsequently, the UV–visible range was adjusted, and peaks were recorded. The size and zeta potential of the NPs were determined using a Zetasizer system (Malvern Zetasizer ZEN 3600, UK) to assess the distribution size of AgNPs and FeNPs in the colloidal solution. The experiment was conducted in triplicate for each nanomaterial from the aqueous honey solution [23].

2.3 Scanning Electron Microscope – Energy Dispersive X-ray (SEM-EDX) Analysis

SEM-EDX analysis was conducted to identify the cellular accumulation of AgNPs and FeNPs, as well as to examine the physical properties including size and shape of honey-treated AgNPs and FeNPs. Samples of honey-mediated AgNPs and FeNPs (25 mL) were centrifuged at 5000 rpm for 10 minutes, washed twice with 0.1X PBS and distilled water, and then freeze-dried. subsequently the freeze-dried honey suspension was then subjected to SEM-EDX analysis (JSM-6701F, Joel, Japan), which generated distinct X-rays representing the elements present in the sample [24].

3. RESULTS

3.1 Biosynthesis and Spectroscopic Characterization of AgNPs and FeNPs

Apis mellifera honey was recognized as a good source for the synthesis of $AgNO_3$NPs and Fe_2O_3NPs. In the present study, $AgNO_3$NPs and Fe_2O_3NPs are produced upon gradual addition, with stirring, of NaOH to a primary solution containing silver and iron salt combined with sodium hydroxide. The development of a golden yellow color and an intense black color provided a visual indication of the presence of nanoparticles in the solution, respectively.

The synthesis of NPs using aqueous honey solutions (AgNPs-H, FeNPs-H) can be confirmed by measuring the surface plasmon resonance (SPR) band using electronic absorption spectroscopy. The ultraviolet-visible (UV–Vis) spectrum of the reaction mixture has an absorption peak, which showed a sharp peak at 400 and 350 nm, confirming the surface plasmon resonance of the synthesized $AgNO_3$NPs and Fe_2O_3NPs, respectively.

3.2 AgNP and FeNP Characterization

The results of the particle size measurement (dynamic light scattering method, DLS), zeta potential (laser Doppler electrophoresis method, ZP) of dispersed particles, and the electrolytic conductivity (EC) of the samples revealed that the AgNPs synthesis increased the peak height at a particle size of the three replicates of each AgNPs: 3546, 2704, and 3097 nm, with an average of 3116 nm. Meanwhile, the average particle size recorded from FeNPs were 1758, 1868, and 1813, with an average of 1813 nm as shown in Fig. (1). Generally, the particle size and zeta potential of NPs significantly affect their various bioactivities.

Accordingly, the zeta potential distributions were monomodal for all samples studied. The synthesis of AgNPs demonstrated an increase in the percentage of scattered light intensity observed in the three replicates of AgNPs, at approximately − 6.826, − 6.487, and − 6.184 mV, with an average of − 6.499 mV, and a zeta deviation of 2.989 mV, with a conductivity of 0.2066 mS/cm. For FeNPs synthesis, the values were 0.5461, -2.343, and -3.159 mV, with an average of -1.625 mV, and a zeta deviation of 4.663 mV, with a conductivity of 0.08528 mS/cm, as shown in Fig. (2).

3.3 AgNPs and FeNPs SEM-EDX Analysis

The (SEM-EDX) was employed to characterize the size, shape, and morphology of AgNPs and FeNPs synthesized at 27°C. An SEM image of AgNPs is shown in Fig 3. The images also revealed the presence of a small number of rod-shaped NPs. These structures can form during synthesis, given that NPs with consistent specific shapes and sizes are difficult to acquire. At 19,000x magnification, the average size of AgNPs measured in the images was 42–55 nm.

The silver (Ag) ions reduced with the addition of NaOH, which acts as a pH regulator. The morphology of AgNPs was obtained from an SEM micrograph. The results indicate that the particle size decreased as the pH of the aqueous solution increased. Therefore, a rapid reduction in Ag ions and the formation of smaller NPs are achieved at higher pH values. The EDX analysis was conducted to examine the elemental composition of the biogenic AgNPs. Oxygen and carbon were the main components revealed by EDX, indicating that the synthesized AgNPs solution contained carbon and oxygen in addition to Ag. This finding was confirmed by the presence of an α peak between 0.0 and 0.83 keV.

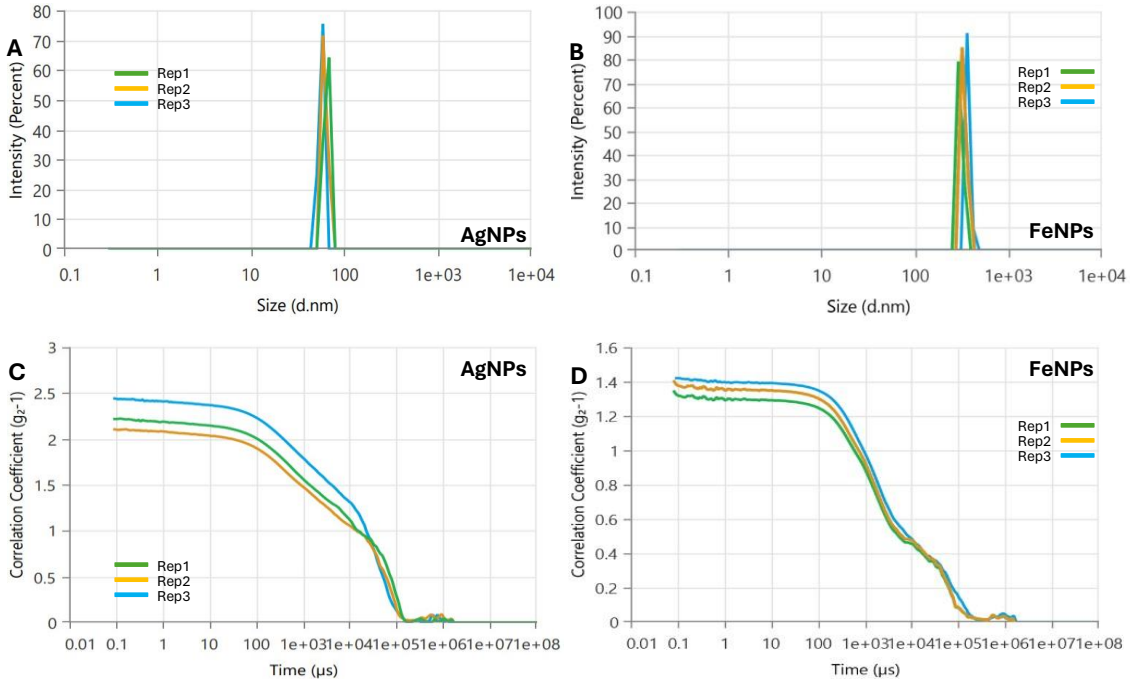

Fig. 1. Mean particle size distribution and correlation of AgNPs (A, C) overtime, and FeNPs (B, D) biosynthesized using commercial honey

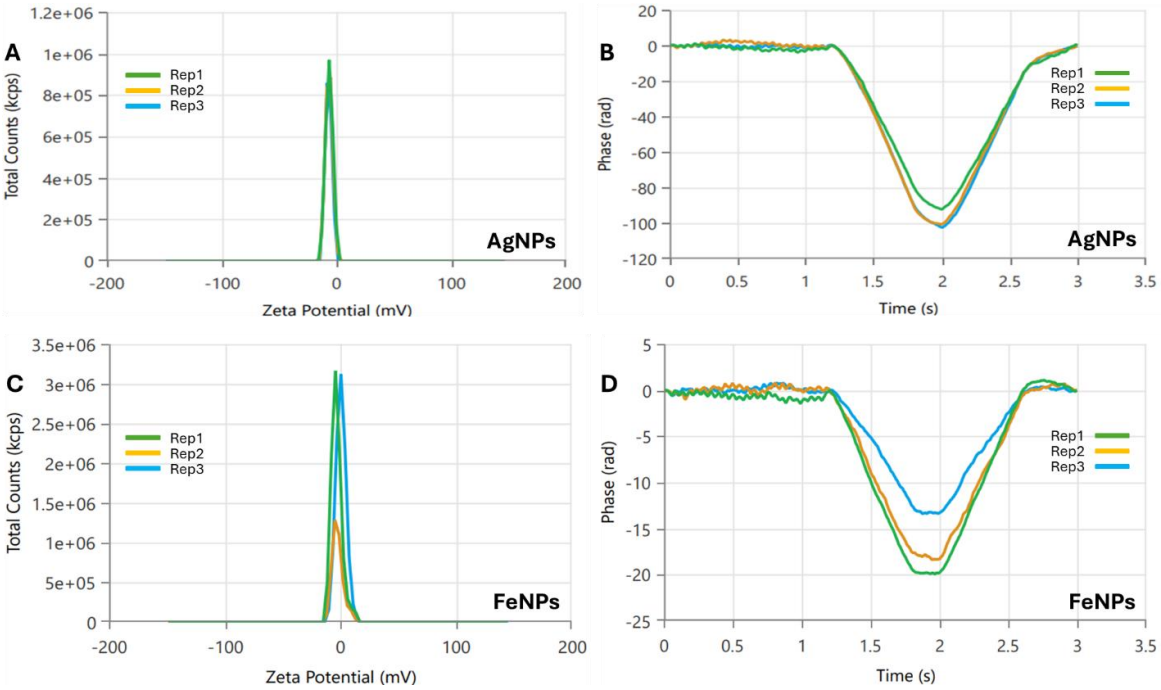

Fig. 2. Mean Zeta potential and phase of AgNPs (A and B over time and FeNPs (C and D) biosynthesized using commercial honey

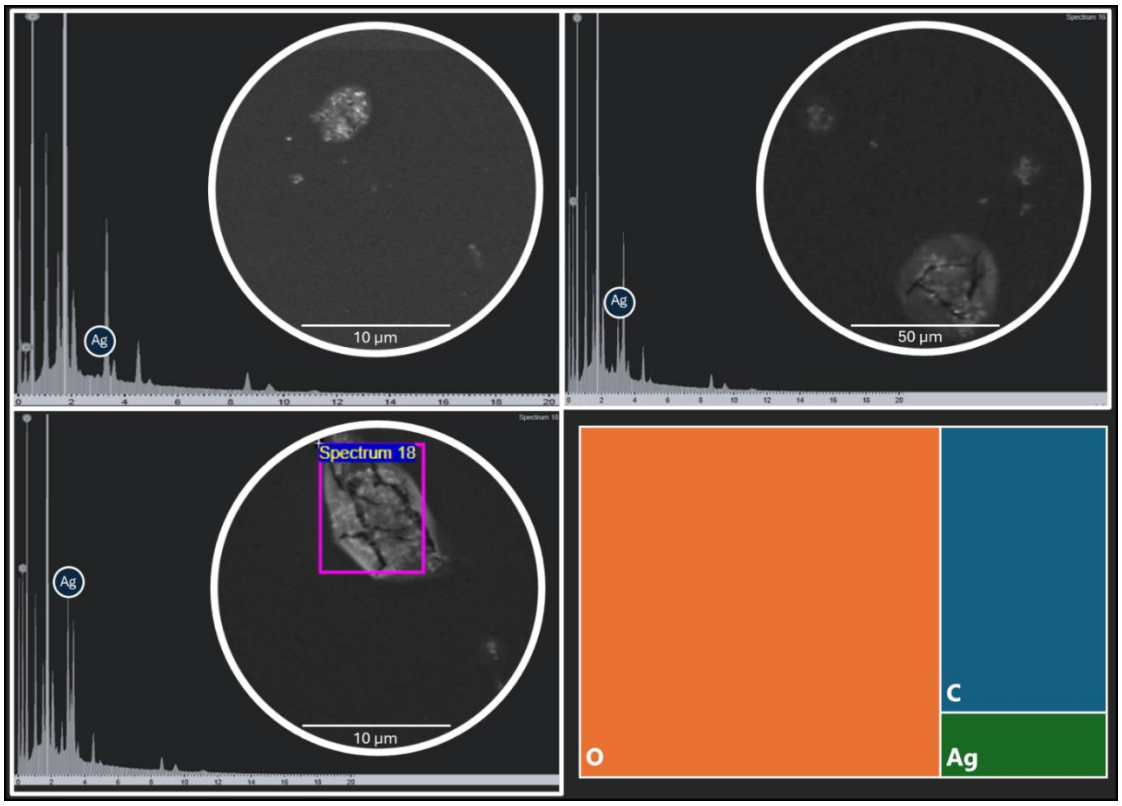

Fig. 3. (Sem-EDX) image for AgNPssynthesized using commercial honey. The boxplot shows the weight % for the Carbon (c), Oxygen (O), and Silver (Ag) content collected from three different scans

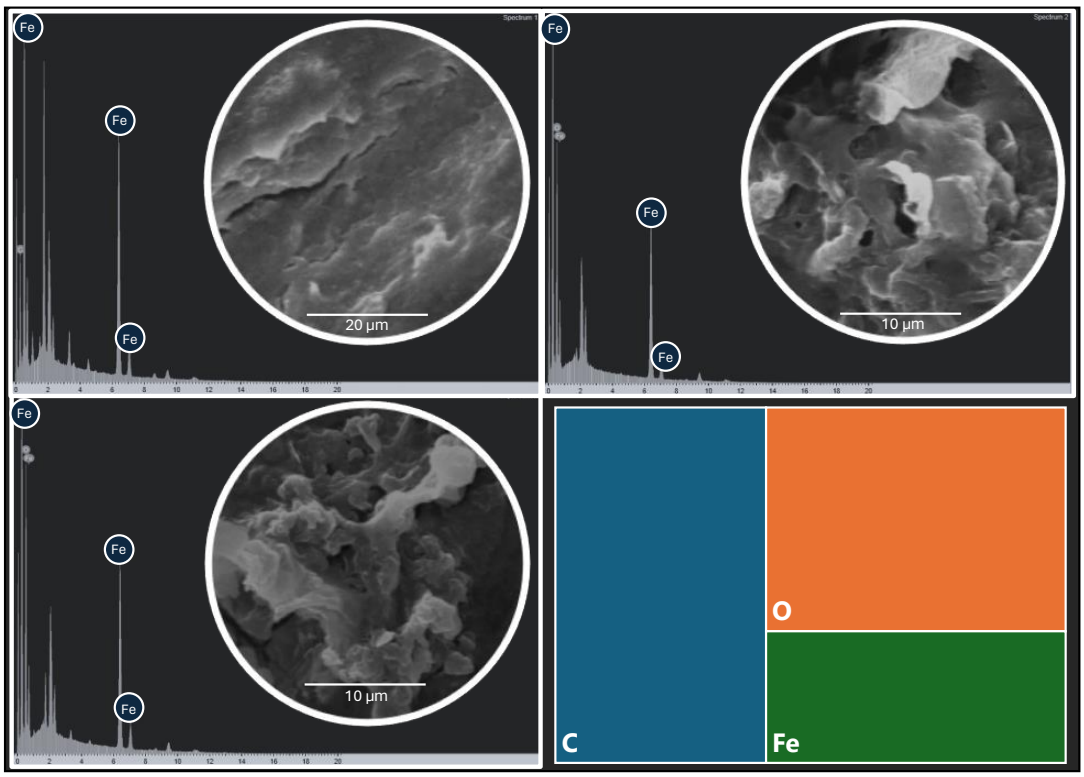

Fig. 4. Sem-EDX image for FeNPssynthesized using commercial honey. The boxplot shows the weight % for the Carbon (c), Oxygen (O), and Iron (Fe) contents collected from three different scans

The morphological (size and shape) properties of the produced FeNPs, as determined by SEM, are depicted in Fig. (4). These images confirmed the development of nanostructures, which were well distributed in the solution. A continuous variation was observed in the shape and size of the produced FeNPs. At 19,000x magnification, the size distribution of FeNPs was approximately in the range of 100–200 nm with a non-uniform spherical shape. The EDX analysis shown in Fig 2c revealed the elemental composition of the synthesized FeNPs solution. α between 0.0 and 0.83 keV confirmed that Fe and O are present in the synthesized NPs. The abundance of oxygen demonstrated that the NPs are in iron oxide form. Peaks of C and O atoms confirmed the contribution of honey in the NP synthesis. The presence of Na and Cl atoms was also detected as impurities in the solution. The highest proportion of Fe elements was found in the EDX spectra, indicating that the main component included Fe_2O_3-NPs.

3.4 Comparative Details between $AgNO_3$ and $Fe2O_3$ NPs

The synthesized $AgNO_3$ exhibited a larger Z-average size (3115.67 nm) than $Fe2O_3$ (1813 nm), indicating a broader size distribution for $AgNO_3$. However, $AgNO_3$ showed a monodisperse particle population with a polydispersity index (PI) of 1, whereas Fe_2O_3 had a slightly broader size distribution with a PI of 0.9492. In terms of mean count rate, $AgNO_3$ demonstrated a higher value (505.17 kcps) than Fe_2O_3 (296.65 kcps), suggesting a higher particle concentration for $AgNO_3$. The peak 1 intensity ordered by area was smaller for $AgNO_3$ (61.36 nm) than for Fe_2O_3 (345.35 nm), indicating a smaller primary particle size for $AgNO_3$.Both NPs displayed negative values for zeta potential, $AgNO_3$ showed a zeta potential of −6.499 mV and Fe_2O_3 exhibiting a slightly higher negative zeta potential of −1.652 mV. The conductivity values were higher for $AgNO_3$ (0.2066 mS/cm) than to Fe_2O_3 (0.08528 mS/cm). Moreover, the wall zeta potential was more negative for $AgNO_3$ (−17.48 mV) than for Fe_2O_3 (−3.182 mV), indicating a stronger charge at the surface of $AgNO_3$ nanoparticles. However, the zeta deviation was higher for Fe_2O_3 (4.663 mV) compared to $AgNO_3$ (2.989 mV), suggesting greater variation in zeta potential measurements for Fe_2O_3. Furthermore, $AgNO_3$ exhibited a significantly higher derived mean count rate

(1673 kcps) than Fe_2O_3 (0.00002802 kcps), indicating a higher overall particle count for $AgNO_3$. However, the reference beam count rate values were similar for both NPs, suggesting comparable measurement accuracy.

In addition to the previously mentioned characterization parameters, the SEM-EDX analysis provided insight into the elemental composition of the NPs. For AgNPs, the average weight percentages were 41.17% for carbon (C), 37.02% for oxygen (O), and 21.80% for iron (Fe). Conversely, FeNPs exhibited an average weight percentage of 19.89% for carbon (C), 73.11% for oxygen (O), and 7.00% for silver (Ag). These elemental composition percentages highlight the differences in the chemical makeup of the two types of NPs. While AgNPs and FeNPs contain carbon and oxygen, indicating the presence of organic and oxide components, respectively, the predominant presence of silver in AgNPs and iron in FeNPs distinguishes their elemental compositions.

4. DISCUSSION

Bio-fabrication of metal NPs using biological resources as capping and stabilizing agents represents a biocompatible, eco-friendly, and nontoxic approach with widespread biomedical applications. Recently, these NPs have drawn considerable attention owing to the magnetic properties and flexible surface chemistry of iron and silver oxide [3,25]. The outcomes from this investigation showed that the addition of bee's honey to the silver in the form of nitrate (1 mM) provided a brown color to the mixture that turned from yellow at the start point of addition, indicating the plasmon resonance excitation of AgNPs [19]. Moreover, the incorporation of iron in the form of an oxide (1 mM) provided an intense black color to the mixture that turned from brown, providing a visual indication of the presence of NPs in the solution. The change in mixture color in a time-dependent manner was observed. After seven days of storage in a dark condition, the dark brown color became clear and stable [21].

UV–VIS spectroscopy was used to observe Ag ions bio-reduction, where peaks of 400 and 350 nm were detected for AgNPs, and FeNPs prepared using bee's honey respectively [26]. During the first stage of the experiment, the synthesis of AgNPs was conducted at a temperature of 25ºC in aqueous honey solutions. A single SPR band indicates that NPs have a spherical shape [27]. The morphology and surface charge of silver and iron were spherical with average diameters of 3115.67 nm and 1813 nm respectively. The negative zeta potential of biogenic AgNPs was −6.499 mV, and −1.651966667 mV for FeNPs. The surface area of the sorbents changed the morphology of the adsorbent particles and showed agglomeration to large shapes [28].

The negative zeta potential of biogenic AgNPs was recorded at -1.625 mV, consistent with the findings of previous studies utilizing honey as a reducing agent [26,29]. This negative zeta potential likely contributes to the stability and uniform distribution of AgNPs by inducing particle repulsion [30]. In addition, negative ionizable groups present in biomolecules from honey may further enhance this negative charge, thereby aiding in AgNPs dispersion of [31]. Conversely, the average zeta potential of FeNPs was measured at −1.625 mV, with a deviation of 4.663 mV. These results suggest that negatively charged groups predominantly constitute the capping biomolecules surrounding the biosynthesized FeNPs [32]. According to Gengan et al. [33], a zeta potential exceeding +30 mV or falling below −30 mV indicates a stable system. However, zeta potentials closer to 0 mV are associated with a higher likelihood of particle agglomeration [34].

The SEM-EDX analysis was conducted to determine the cellular accumulation of AgNPs and FeNPs in the aqueous honey solution resulting from the NP treatment. The SEM images with a magnification of up to 20,000x revealed that the AgNP and FeNP size distribution were in the range of 100 and 200 nm respectively. SEM-ED images showed that AgNPs reveal spherical shapes and uniform NP distributions , with smooth edges, and without any aggregation observed. The EDX spectrometers have confirmed the presence Ag signal in the synthesized AgNPs. The percentage of Ag metal found other chemical elements was substantial, at approximately 7%. SEM-EDX was used for element analysis of the biogenic AgNPs prepared in the current study showing the oxygen and carbon as the main components. AgNPs nanostructure prepared from honey and contains carbon and oxygen besides the Ag was also discussed by El-Deeb et al. [35]. The other elements that originated from honey ingredients such as glucose, fructose, organic acids, vitamins, and minerals served as capping organic agents bound to the AgNP surface

[36,37]. Previous similar studies stated that AgNPs particles with the same shape and characteristics obtained by bee's honey collected from different floral sources where SEM and transition electron microscopy (TEM) analysis were used [35,38]. Recent studies have also demonstrated that the size of iron oxide-based NPs is between 10 and 100 nm [39,40].

In this study, the shape of FeNPs was irregularly spherical. A previous study also reported a cavity-like shape with a rough surface of FeNPs [41]. The SEM images of the present study revealed that the precursor (honey) stabilized the NP surface of by selectively slowing their growth rate and stopping particle aggregation. This result can be correlated with a previous similar study [42]. Another study demonstrated that the nature of FeNPs was not uniform and that they were present mostly in the form of large, agglomerated groups. These clusters were linked to the low capping ability of the plant source and the magnetic properties of FeNPs [22].

The EDX analysis was performed to determine the elemental content of the sample. Iron typically exhibits an intense peak at 0.7–7 keV [43]. The presence of carbon and oxygen, together with iron, confirmed the involvement of honey in the synthesis of NP structures. This condtion achieved quantitative and qualitative evaluations of the iron components thereby generating FeNPs [44]. Cl and Na atoms were also found as residual impurities while synthesizing NPs from ferric chloride.This finding has been documented in previous studies [45].

5. CONCLUSION

A fast, eco-friendly, and convenient green method was used to synthesize AgNPs and FeNPs using honey. The current study presents detailed results of a bio-reductive green synthesis of AgNPs, FeNPs using bee honey. Honey was demonstrated to be effective in reducing and capping agents to produce stable and well-dispersed AgNPs and FeNPs. NP formation was investigated by UV-vis, zeta potential, and SEM-EDX analysis. The characterization results of AgNPs and FeNPs reveal notable distinctions between the two materials. AgNPs exhibit a larger particle size, higher particle concentration, and a more negative zeta potential than FeNPs. In addition, AgNPs display a monodisperse particle population with a broader size distribution, whereas FeNPs show a slightly broader size distribution. Furthermore, SEM-EDX analysis elucidates the elemental composition of AgNPs and FeNPs, with AgNPs primarily consisting of silver, carbon, and oxygen, whereas FeNPs predominantly comprise iron, oxygen, and carbon. These findings underscore the distinct characteristics and compositions of AgNPs and FeNPs, highlighting their potential applications in various fields.

CONSENT

It is not applicable.

ETHICAL APPROVAL

It is not applicable.

COMPETING INTERESTS

Author has declared that no competing interests exist.

REFERENCES

1. Rostamizadeh E, Iranbakhsh A, Majd A, Arbabian S, Mehregan I. Green synthesis of Fe_2O_3 nanoparticles using fruit extract of *Cornus mas* L. and its growth-promoting roles in Barley. J Nanostruct Chem. 2020;10(2):125-130. DOI:10.1007/s40097-020-00335-z
2. Iravani S, Korbekandi H, Mirmohammadi SV, Zolfaghari B. Synthesis of silver nanoparticles: chemical, physical and biological methods. Res Pharm Sci. 2014;9(6):385-406.
3. Galúcio JMP, De Souza SGB, Vasconcelos AA, et al. Synthesis, Characterization, Applications, and Toxicity of Green Synthesized Nanoparticles. CPB. 2022;23(3):420-443. DOI:10.2174/1389201022666210521102307
4. Mohammadzadeh V, Barani M, Amiri MS, et al. Applications of plant-based nanoparticles in nanomedicine: A review. Sustainable Chemistry and Pharmacy. 2022;25:100606. DOI: 10.1016/j.scp.2022.100606
5. Nagajyothi PC, Pandurangan M, Kim DH, Sreekanth TVM, Shim J. Green Synthesis of Iron Oxide Nanoparticles and Their Catalytic and *In vitro* Anticancer Activities. J Clust Sci. 2017;28(1):245-257. DOI: 10.1007/s10876-016-1082-z

6. Jamkhande PG, Ghule NW, Bamer AH, Kalaskar MG. Metal nanoparticles synthesis: An overview on methods of preparation, advantages and disadvantages, and applications. Journal of Drug Delivery Science and Technology. 2019;53:101174.
DOI: 10.1016/j.jddst.2019.101174
7. Rathod S, Preetam S, Pandey C, Bera SP. Exploring synthesis and applications of green nanoparticles and the role of nanotechnology in wastewater treatment. Biotechnology Reports. 2024; 41:e00830.
DOI: 10.1016/j.btre.2024.e00830
8. Chugh D, Viswamalya VS, Das B. Green synthesis of silver nanoparticles with algae and the importance of capping agents in the process. Journal of Genetic Engineering and Biotechnology. 2021;19 (1):126.
DOI: 10.1186/s43141-021-00228-w
9. Shah AA, Bhatti MA, Tahira A, et al. Facile synthesis of copper doped ZnO nanorods for the efficient photo degradation of methylene blue and methyl orange. Ceramics International. 2020;46(8):9997-10005.
DOI: 10.1016/j.ceramint.2019.12.024
10. Gopu M, Kumar P, Selvankumar T, et al. Green biomimetic silver nanoparticles utilizing the red algae Amphiroa rigida and its potent antibacterial, cytotoxicity and larvicidal efficiency. Bioprocess Biosyst Eng. 2021;44(2):217-223.
DOI: 10.1007/s00449-020-02426-1
11. Üstün E, Önbaş SC, Çelik SK, Ayvaz MÇ, Şahin N. Green Synthesis of Iron Oxide Nanoparticles by Using Ficus Carica Leaf Extract and Its Antioxidant Activity. Biointerface Res Appl Chem. 2021;12(2): 2108-2116.
doi:10.33263/BRIAC122.21082116
12. González Fá AJ, Juan A, Di Nezio MS. Synthesis and Characterization of Silver Nanoparticles Prepared with Honey: The Role of Carbohydrates. Analytical Letters. 2017;50(5):877-888.
DOI: 10.1080/00032719.2016.1199558
13. Behravan M, Hossein Panahi A, Naghizadeh A, Ziaee M, Mahdavi R, Mirzapour A. Facile green synthesis of silver nanoparticles using Berberis vulgaris leaf and root aqueous extract and its antibacterial activity. International Journal of Biological Macromolecules. 2019;124: 148-154.
DOI: 10.1016/j.ijbiomac.2018.11.101
14. Rasheed T, Bilal M, Iqbal HMN, Li C. Green biosynthesis of silver nanoparticles using leaves extract of Artemisia vulgaris and their potential biomedical applications. Colloids and Surfaces B: Biointerfaces. 2017;158:408-415.
DOI: 10.1016/j.colsurfb.2017.07.020
15. Aboyewa JA, Sibuyi NRS, Meyer M, Oguntibeju OO. Green Synthesis of Metallic Nanoparticles Using Some Selected Medicinal Plants from Southern Africa and Their Biological Applications. Plants. 2021;10(9):1929.
DOI: 10.3390/plants10091929
16. Varadavenkatesan T, Selvaraj R, Vinayagam R. Phyto-synthesis of silver nanoparticles from Mussaenda erythrophylla leaf extract and their application in catalytic degradation of methyl orange dye. Journal of Molecular Liquids. 2016;221:1063-1070.
DOI: 10.1016/j.molliq.2016.06.064
17. Tufani A, Qureshi A, Niazi JH. Iron oxide nanoparticles based magnetic luminescent quantum dots (MQDs) synthesis and biomedical/biological applications: A review. Materials Science and Engineering: C. 2021;118:111545.
DOI: 10.1016/j.msec.2020.111545
18. Ali I, Pan Y, Jamil Y, et al. Comparison of copper-based Cu-Ni and Cu-Fe nanoparticles synthesized via laser ablation for magnetic hyperthermia and antibacterial applications. *Physica B:* Condensed Matter. 2023;650:414503.
DOI: 10.1016/j.physb.2022.414503
19. Keskin M, Kaya G, Keskin S. Nanotechnology in Honey: Future and Perspectives Honey as Nanoparticles. In: Bhattacharya T, Ahmed S, eds. Nanotechnology in Functional Foods. 1st ed. Wiley. 2022:87-101.
DOI: 10.1002/9781119905059.ch4
20. Haiza H, Azizan A, Mohidin AH, Halin DSC. Green Synthesis of Silver Nanoparticles Using Local Honey. *NH*. 2013;4:87-98.
doi:10.4028/www.scientific.net/NH.4.87
21. Shahid H, Shah AA, Shah Bukhari SNU, et al. Synthesis, Characterization, and Biological Properties of Iron Oxide Nanoparticles Synthesized from Apis mellifera Honey. *Molecules*. 2023;28(18): 6504.
DOI: 10.3390/molecules28186504

22. Bhuiyan MdSH, Miah MY, Paul SC, et al. Green synthesis of iron oxide nanoparticle using Carica papaya leaf extract: application for photocatalytic degradation of remazol yellow RR dye and antibacterial activity. Heliyon. 2020;6(8):e04603. DOI: 10.1016/j.heliyon.2020.e04603
23. Abd El-Aziz ARM, Al-Othman MR. Biosynthesized gold nanoparticles using Zingiber officinale and its impact on the growth and chemical composition of lentils (Lens culinaris). PAKJBOT. 2019;51(2). DOI: 10.30848/PJB2019-2(21)
24. Scimeca M, Bischetti S, Lamsira HK, Bonfiglio R, Bonanno E. Energy Dispersive X-ray (EDX) microanalysis: A powerful tool in biomedical research and diagnosis. *Eur J Histochem*. Published; 2018. DOI: 10.4081/ejh.2018.2841
25. Priya, Naveen, Kaur K, Sidhu AK. Green Synthesis: An Eco-friendly Route for the Synthesis of Iron Oxide Nanoparticles. Front Nanotechnol. 2021;3:655062. DOI: 10.3389/fnano.2021.655062
26. El-Desouky T, Ammar H. Honey mediated silver nanoparticles and their inhibitory effect on aflatoxins and ochratoxin A. *J App Pharm Sci*. Published online 2016: 083-090. DOI: 10.7324/JAPS.2016.60615
27. Wan Y, Guo Z, Jiang X, et al. Quasi-spherical silver nanoparticles: Aqueous synthesis and size control by the seed-mediated Lee–Meisel method. Journal of Colloid and Interface Science. 2013;394: 263-268. DOI: 10.1016/j.jcis.2012.12.037
28. Kumar R, Goswami S, Rai GK, et al. Protection from terminal heat stress: a trade-off between heat-responsive transcription factors (HSFs) and stress-associated genes (SAGs) under changing environment. Cereal Research Communications. 2020;49(2):227-234. DOI: 10/gsm75g
29. Mohammed A, Al-Qahtani A, al-Mutairi A, Al-Shamri B, Aabed K. Antibacterial and Cytotoxic Potential of Biosynthesized Silver Nanoparticles by Some Plant Extracts. Nanomaterials. 2018;8(6):382. DOI: 10.3390/nano8060382
30. Farhadi S, Ajerloo B, Mohammadi A. Green Biosynthesis of Spherical Silver Nanoparticles by Using Date Palm (Phoenix Dactylifera) Fruit Extract and Study of Their Antibacterial and Catalytic Activities. *Acta Chim Slov*; 129-143. DOI: 10.17344/acsi.2016.2956
31. Khatoon N, Mazumder JA, Sardar M. Biotechnological Applications of Green Synthesized Silver Nanoparticles. J Nanosci Curr Res. 2017;02(01). DOI: 10.4172/2572-0813.1000107
32. Balasooriya ER, Jayasinghe CD, Jayawardena UA, Ruwanthika RWD, Mendis De Silva R, Udagama PV. Honey Mediated Green Synthesis of Nanoparticles: New Era of Safe Nanotechnology. Journal of Nanomaterials. 2017;2017:1-10. DOI: 10.1155/2017/5919836
33. Gengan RM, Anand K, Phulukdaree A, Chuturgoon A. A549 lung cell line activity of biosynthesized silver nanoparticles using Albizia adianthifolia leaf. *Colloids and Surfaces B: Biointerfaces*. 2013;105: 87-91. DOI: 10.1016/j.colsurfb.2012.12.044
34. Guo Y, Zhao Y, Wang S, Jiang C, Zhang J. Relationship between the zeta potential and the chemical agglomeration efficiency of fine particles in flue gas during coal combustion. Fuel. 2018;215:756 -765. DOI: 10.1016/j.fuel.2017.11.005
35. El-Deeb N, El-Sherbiny I, El-Aassar M, Hafez E. Novel Trend in Colon Cancer Therapy Using Silver Nanoparticles Synthesized by Honey Bee. J Nanomed Nanotechnol. 2015;06(02). DOI: 10.4172/2157-7439.1000265
36. Femi-Adepoju AG, Dada AO, Otun KO, Adepoju AO, Fatoba OP. Green synthesis of silver nanoparticles using terrestrial fern (Gleichenia Pectinata (Willd.) C. Presl.): characterization and antimicrobial studies. Heliyon. 2019;5(4): e01543. DOI: 10.1016/j.heliyon.2019.e01543
37. Matar GH, Akyüz G, Kaymazlar E, Andac M. An Investigation of Green Synthesis of Silver Nanoparticles Using Turkish Honey Against Pathogenic Bacterial Strains. *Biointerface* Res Appl Chem. 2022;13(2): 195. DOI: 10.33263/BRIAC132.195
38. Hosny AMS, Kashef MT, Rasmy SA, Aboul-Magd DS, El-Bazza ZE. Antimicrobial activity of silver nanoparticles synthesized using honey and gamma radiation against silver-resistant bacteria from wounds and burns. Adv Nat Sci: Nanosci Nanotechnol. 2017;8(4):045009. DOI: 10.1088/2043-6254/aa8b44

39. Miri A, Najafzadeh H, Darroudi M, Miri MJ, Kouhbanani MAJ, Sarani M. Iron Oxide Nanoparticles: Biosynthesis, Magnetic Behavior, Cytotoxic Effect. Chemistry Open. 2021;10(3):327-333. DOI: 10.1002/open.202000186
40. Salama AM, Abedin RMA, Elwakeel KZ. Influences of greenly synthesized iron oxide nanoparticles on the bioremediation of dairy effluent using selected microbial isolates. Int J Environ Sci Technol. 2022; 19(8):7019-7030. DOI: 10.1007/s13762-021-03625-3
41. Ahmad W, Kumar Jaiswal K, Amjad M. *Euphorbia herita* leaf extract as a reducing agent in a facile green synthesis of iron oxide nanoparticles and antimicrobial activity evaluation. Inorganic and Nano-Metal Chemistry. 2020:1-8. DOI: 10.1080/24701556.2020.1815062
42. Sharmila M, Mani RJ, Parvathiraja C, et al. Photocatalytic Dye Degradation and Bio-Insights of Honey-Produced α-Fe_2O_3 Nanoparticles. Water. 2022;14(15):2301. DOI: 10.3390/w14152301
43. Biswas A, Vanlalveni C, Lalfakzuala R, Nath S, Rokhum SL. Mikania mikrantha leaf extract mediated biogenic synthesis of magnetic iron oxide nanoparticles: Characterization and its antimicrobial activity study. Materials Today: Proceedings. 2021;42:1366-1373. DOI: 10.1016/j.matpr.2021.01.108
44. Menazea AA, Ahmed MK. Silver and copper oxide nanoparticles-decorated graphene oxide via pulsed laser ablation technique: Preparation, characterization, and photoactivated antibacterial activity. Nano-Structures & Nano-Objects. 2020;22: 100464. DOI: 10.1016/j.nanoso.2020.100464
45. Qasim S, Zafar A, Saif MS, et al. Green synthesis of iron oxide nanorods using Withania coagulans extract improved photocatalytic degradation and antimicrobial activity. Journal of Photochemistry and Photobiology B: Biology. 2020;204:111784. DOI: 10.1016/j.jphotobiol.2020.111784

Peer-review history:
The peer review history for this paper can be accessed here:
https://www.sdiarticle5.com/review-history/116383